CDF/ANAL/TOP/PUBLIC/9114

Measurement of the W Helicity in Fully Reconstructed Top Anti-Top Events using 1.9 fb^{-1}

Thorsten Chwalek, Dominic Hirschbühl, Thomas Muller, Jeannine Wagner-Kuhr, Wolfgang Wagner

Abstract

We present a measurement of the fraction of longitudinally (F_0) polarized and right-handed (F_+) W bosons in top quark decays in the lepton+jets channel. The analyzed dataset corresponds to an integrated luminosity of about 1.9 fb^{-1}. As sensitive observable we use the cosine of the decay angle θ^* of the charged lepton in the W rest frame measured with respect to the direction of motion of the W boson in the top-quark rest-frame. In order to determine the $\cos\theta^*$ distribution in the data, the kinematics of the $t\bar{t}$ events are fully reconstructed. We find $F_0 =$ 0.66 ± 0.10 (stat) $\pm$0.06 (syst) (with F_+ fixed to zero) and $F_+ = 0.01$ ± 0.05 (stat) $\pm$0.03 (syst) (with F_0 fixed to 0.7). Fitting both fractions simultaneously we find $F_0 = 0.38$ ± 0.21 (stat) $\pm$0.07 (syst) and $F_+ = 0.15$ ± 0.10 (stat) $\pm$0.05 (syst).

1 Introduction

Since the discovery of the top quark in 1995 by the CDF and DØ collaborations [1], the mass of this most massive known elementary particle has been measured with high precision. However, the measurements of other top-quark properties are still statistically limited, so the question remains whether the standard model successfully predicts these properties. In the following we present our measurement of the helicity fractions of the W bosons from the top-quark decay.

At the Tevatron collider, with a center-of-mass energy of 1.96 TeV, most top quarks are pair-produced via the strong interaction. In the standard model the top quark decays in nearly 100% of all cases into a W boson and a b quark. Due to its large mass the top quark has a lifetime, that is shorter than the hadronization time. Thus its decay products preserve the helicity content of the underlying weak interaction.

In this analysis, the structure of the weak interaction is investigated by measuring the helicity fractions of the W boson in top quark decays. In order to discuss which couplings in the Wtb vertex could have an impact on the W helicity fractions, the interaction Lagrangian [2] for the most general coupling is considered. The interaction of fermions and gauge bosons in general, can be expressed by six form factors with a particular energy scale at which new physics is opened. Assuming the W boson to be on-shell, the number of the form factors can be reduced to four:

$$L = \frac{g}{\sqrt{2}}[W_\mu^- \bar{b}\gamma^\mu(f_1^L P_- + f_1^R P_+)t - \frac{1}{m_W}\partial_\nu W_\mu^- \bar{b}\sigma^{\mu\nu}(f_2^L P_- + f_2^R P_+)t] + cc \qquad (1)$$

with

$$i\sigma^{\mu\nu} = -\frac{1}{2}[\gamma^\mu, \gamma^\nu]. \qquad (2)$$

In the standard model of elementary particle physics f_1^L is equal to one, while the three other form factors $(f_1^R, f_2^{R,L})$ are all equal to zero, leading to a pure $V-A$ structure of the weak interaction. This $V-A$ structure predicts that the W bosons from the top-quark decay are dominantly either longitudinally polarized or left-handed, while right-handed W bosons are heavily suppressed and even forbidden in the limit of a massless b quark. The fraction of longitudinally polarized W bosons is given by [2]:

$$F_0 = \frac{\Gamma(t \to W_0 b)}{\Gamma(t \to W_0 b) + \Gamma(t \to W_\pm b)} = \frac{1/2(m_t/m_W)^2}{1/2(m_t/m_W)^2 + 1} = \frac{m_t^2}{2M_W^2 + m_t^2}, \qquad (3)$$

where the b quark mass has been neglected. Assuming a top-quark mass of 175 GeV/c^2, the fraction of longitudinally polarized W bosons is predicted [2] to be $F_0 = 0.7$, while the fraction of left-handed W bosons is $F_- = 0.3$. A significant deviation from the predicted value for F_0 or a nonzero value for the right-handed fraction F_+ could indicate new physics, such as a possible $V + A$ component in the weak interaction or other anomalous couplings at the Wtb vertex.

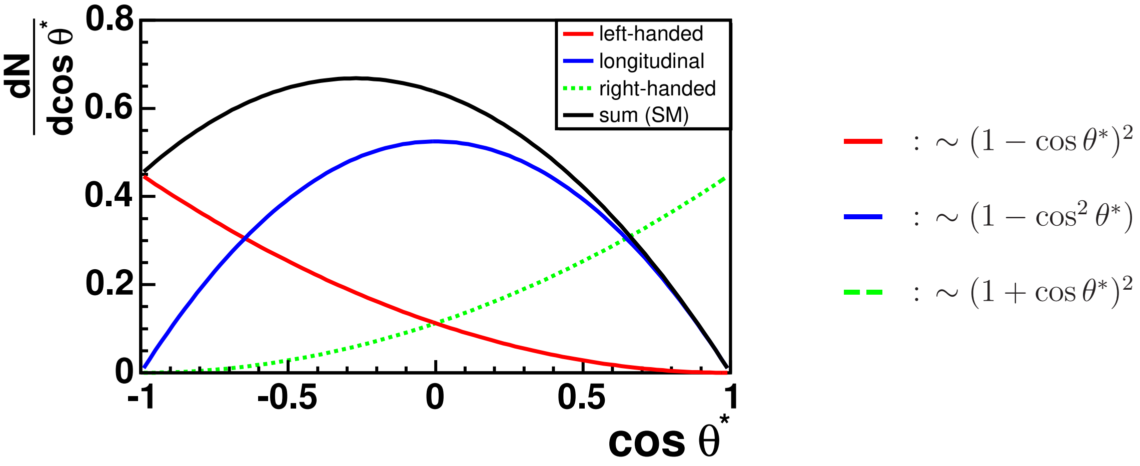

Figure 1: Theoretically calculated $\cos\theta^*$ distributions for left-handed (red), longitudinally (blue) and right-handed (green dashed) polarized W-bosons. The solid black line indicates the $\cos\theta^*$ distribution as expected in the standard model.

The W boson polarization manifests itself in the decay $W \to \ell\nu_\ell$ in the angle θ^*, which is defined as the angle between the momentum of the charged lepton in the W rest frame and the momentum of the W boson in the top-quark rest-frame. The general $\cos\theta^*$ distribution is given by [2]:

$$\frac{dN}{d\cos\theta^*} \propto F_- \cdot \frac{3}{8}(1-\cos\theta^*)^2 + F_0 \cdot \frac{3}{4}(1-\cos^2\theta^*) + F_+ \cdot \frac{3}{8}(1+\cos\theta^*)^2 \tag{4}$$

The $\cos\theta^*$ distributions for the three helicity modes as well as for the standard model expectation, are presented in figure 1.

In order to measure the W helicity content in top quark decays we select top anti-top events in the lepton+jets channel, reconstruct the four-vectors of the top quarks and W bosons and calculate $\cos\theta^*$ of the semileptonically decaying top quark for each $t\bar{t}$ event. We then extract the longitudinal fraction F_0 and the right-handed fraction F_+ from the reconstructed $\cos\theta^*$ distribution using a binned maximum likelihood fit. The signal templates used for this fit are calculated from first principle and corrected for detector effects using Monte Carlo generated events.

2 The CDF II Experiment

A detailed description of the Collider Detector at Fermilab (CDF) can be found elsewhere [3]. A coordinate system with the z axis along the proton beam, azimuthal angle ϕ, and polar angle θ is used. The pseudorapidity is defined as $\eta = -\ln\tan(\theta/2)$. The transverse energy of a particle is defined as $E_T = E\sin\theta$. The primary detector components relevant to this analysis are those that measure the jet, electron, and muon energies and directions.

An open cell drift chamber, the Central Outer Tracker (COT), and a silicon tracking system are used to measure the momenta of charged particles. The CDF II silicon tracker consists of three subdetector: (1) a layer of single-sided radiation resistant silicon microstrip detectors glued on the beam pipe, (2) a five layer double-sided silicon microstrip detector (SVXII), and (3) additional Intermediate Silicon Layers located at radii between 19 and 30 cm provide good linking between the track segments in the COT and the SVXII. In the analysis presented in this paper the silicon tracker is particularly important to identify jets originating from b quarks by reconstructing secondary vertices. The tracking chambers are all located within a 1.4 T axial magnetic field. The pseudorapidity coverage of the COT is $|\eta| < 1.1$, while the silicon system reaches up the $|\eta| < 2.0$. All electromagnetic and hadronic calorimeters at CDF are used to measure the jets energy. In this analysis jets are reconstructed in the pseudorapidity range of $|\eta| < 2.0$. The Central Electromagnetic and Central Hadronic Calorimeter with an angular coverage of $|\eta| < 1.1$ are used to identify electron candidates. The Central Muon System, Central Muon Upgrade, and the Central Muon Extension, with a total coverage of $|\eta| < 1.0$ are used to identify muons.

3 Event Selection of $t\bar{t}$ Candidates

We select $t\bar{t}$ candidate events, where one top quark decays semileptonically, $t \rightarrow b\ell\nu$, and the second top quark decays hadronically, $\bar{t} \rightarrow \bar{b}q\bar{q}'$. The charged lepton is either identified as an electron or muon candidate. The branching ratio of this lepton + jets channel is about 30%.

Top quark candidates in the lepton + jets channel are selected by requiring evidence for a leptonic W decay: (a) missing transverse energy $\not\!\!E_T > 20$ GeV from the neutrino and (b) exactly one well isolated central electron candidate with $E_T > 20\,\text{GeV}$ and $|\eta| < 1.1$, or exactly one well isolated central muon candidate with $p_{\text{T}} > 20\,\text{GeV}/c$ and $|\eta| < 1.0$. An electron or muon candidate is considered isolated if the non-lepton E_T in an $\eta - \phi$ cone of radius 0.4 centered around the lepton is less than 10% of the lepton E_T or p_T, respectively. Jets are reconstructed using a fixed cone of radius $\Delta R = \sqrt{\Delta\phi^2 + \Delta\eta^2} = 0.4$. We count jets with $E_T > 20$ GeV and with a pseudorapidity of $|\eta| < 2.0$. Only events with at least four jets are accepted. Because in $t\bar{t}$ events two b jets should exist, we require, that at least one of these jets must be likely to originate from a b quark (b-tag) by requiring a displaced secondary vertex within the jet as measured using silicon tracker information. Altogether we select 484 $t\bar{t}$ candidate events.

4 Signal Simulation and Background Estimation

Monte Carlo simulations are used to determine the efficiencies and resolution due to the reconstruction of top-pair signal events. All generated events are passed through the CDF detector simulation. Afterwards the same reconstruction as for real data is applied.

The $t\bar{t}$ signal sample is generated with the Monte Carlo generator PYTHIA [4] using a top mass of $m_t = 175$ GeV/c^2.

The selected $t\bar{t}$ candidates in data still contain some background contamination. We observe 484 events with an background estimation of 86.53 events. One source of background events are W-boson plus jets events. Here two different types of W-production have to be distinguished. The first category are W events, where the jets originate from light quarks. In this case one jet is misidentified as a b-quark jet (mistags). The second category are W events with one or more jets originating from a c- or b-quark (W + heavy flavor events). A further source of background are QCD processes, where one jet fakes the charged lepton and another jet is misidentified as a b-quark jet. This background is called QCD background or non-W background. In addition electroweak processes, like di-boson (ZW, WW, ZZ) and single top production contribute to the background. However, the fraction of these backgrounds is rather small and can be determined from the Monte-Carlo simulation.

5 Full Reconstruction of Top Anti-Top Pairs

Due to the incomplete measurement of the neutrino four momentum and several possibilities to assign the jets to the decay products of the top quarks the reconstruction of $t\bar{t}$ pairs has to handle with several possible event hypotheses. For the reconstruction of $t\bar{t}$ events the selected jets and the missing transverse energy are corrected to parton level.

Both top quarks are reconstructed from the measured four momenta of their decay particles. Since the neutrino does not interact with the detector, it appears only in the missing transverse energy. Thus only the x and y component of the neutrino momentum are known. The missing z component is calculated using a W mass constraint on the W boson decay. This treatment leads to a quadratic equation for p_z of the neutrino. In 70% of all cases this results in an ambiguity of two real solutions for $p_{z,\nu}$, which have both to be taken into account. In the remaining 30% of events the solution of the quadratic equation becomes complex. In these cases we vary the x and y component starting from the measured values until the the imaginary part of the p_z solution vanishes. Thus this treatment leads in this cases to only one solution for the z component of the neutrino momentum.

We consider all possibilities to assign the jets in the event to the two b quarks and the two light quarks from the $t\bar{t}$ decay. It should also be mentioned that we take all jets of the event into account and not only the four leading jets. This procedure leads to a multiplicity of possibilities for the reconstruction of the event. Due to the N_ν (2 or 1) solutions for the z-component of the momentum of the neutrino and the $N_{jets} \cdot (N_{jets} - 1) \cdot (N_{jets} - 2)/2 \cdot (N_{jets} - 3)$ ways to assign the selected jets to the four jets in the $t\bar{t}$ decay, $N_\nu \cdot N_{jets} \cdot (N_{jets} - 1) \cdot (N_{jets} - 2) \cdot (N_{jets} - 3)/2$ hypotheses for the complete kinematic reconstruction of a $t\bar{t}$ event candidate are obtained.

In order to choose the best event interpretation, a quantity Ψ is determined for each hypothesis, which gives a quantitative estimate how well the hypothesis matches the $t\bar{t}$

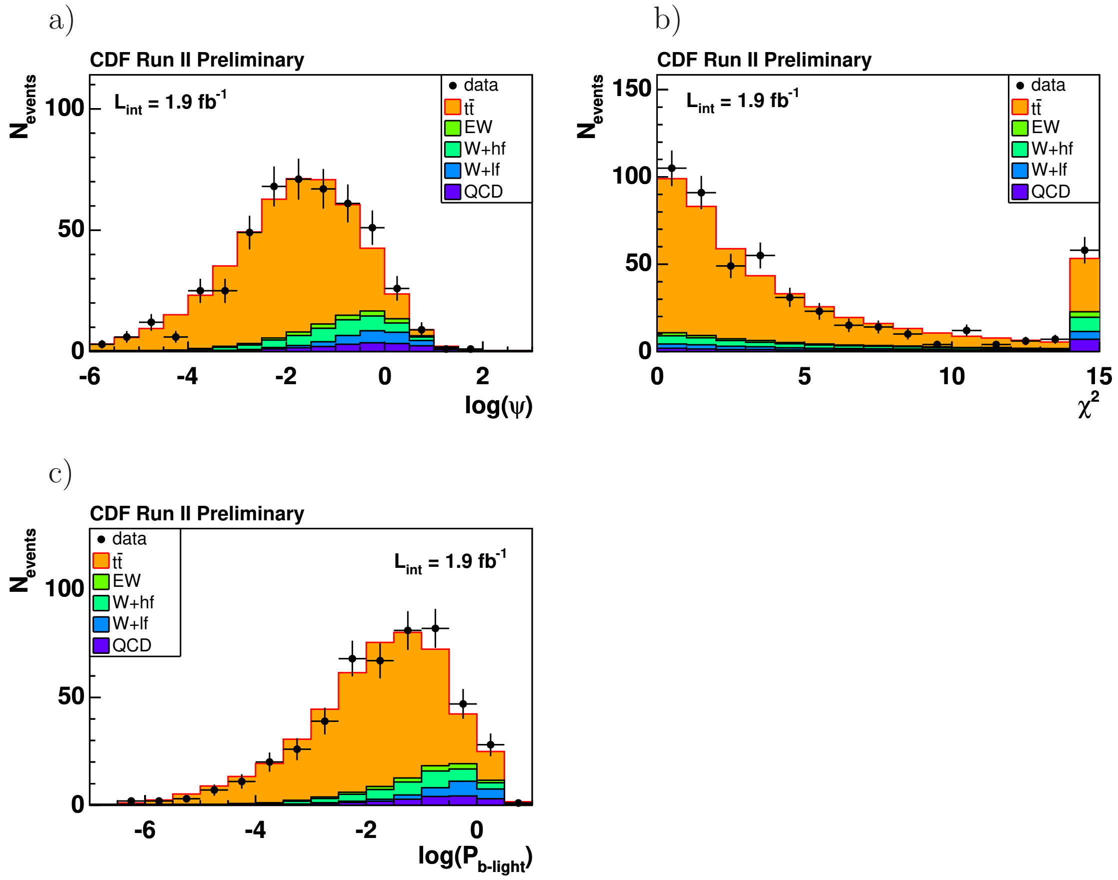

Figure 2: Data-MC comparison for the quantity Ψ and its main ingredients χ^2 and $P_{\mathrm{b-light}}$. Since the values of Ψ and $P_{\mathrm{b-light}}$ cover a wide range, the logarithm of theses quantities is shown.

pair assumption. Ψ is defined by:

$$\Psi = P_\nu \cdot P_{\mathrm{b-light}} \cdot \chi^2 \tag{5}$$

The several quantities entering the computation of Ψ are:

P_ν is a weighting factor for the chosen z component solution of the four-vector of the neutrino, taking into account that in case of two real solutions the one with the smaller absolute value is in 70% of all cases the correct one.

$P_{\mathrm{b-light}}$ is a measure for the light quark likeness of the jets assigned to the b quarks from the top decays and is defined as:

$$P_{b-light} \;=\; (JP_{top\rightarrow b\ell\nu} + (1 - R'_{top\rightarrow b\ell\nu})) \cdot (JP_{top\rightarrow bjj} + (1 - R'_{top\rightarrow bjj})) \tag{6}$$

Here $JP_{top\rightarrow bl\nu}$ and $JP_{top\rightarrow bjj}$ are the probability of the jet [5] chosen to be the b jet from the semileptonically and hadronically decaying top quark, respectively, to be consistent with a zero lifetime hypothesis, i.e. to be a light quark jet. This probability is calculated from the positive impact parameter in the $r-\phi$-plane of the tracks assigned to the jet. For jets with a well displaced secondary vertex a more accurate b-likeness measure R' is calculated using the output of a neural network b-tagger (the KIT flavor separator [6]), while R' is set to zero otherwise. Since $P_{b-light}$ is defined as the probability for the assigned b jets to be light quark jets, we have to use (1-R') instead of R' in equation 6.

Constraints on the mass of the hadronically decaying W boson, on the mass difference between both reconstructed top masses (two particles with the same mass), and on the transverse energy of the two top quarks are combined in the factor χ^2 which is defined via:

$$\chi^2 = \frac{(m_{W\to jj}-M_{W\to jj})^2}{\sigma^2_{M_{W\to jj}}} + \frac{(m_{top\to b\ell\nu}-m_{top\to bjj})^2}{\sigma^2_{\Delta M_t}} + \frac{(P_{energy}-\alpha)^2}{\sigma^2_{P_{energy}}} \tag{7}$$

In the first term $m_{W\to jj}$ is the reconstructed mass of the hadronically decaying W boson, which should be equal to the mean value $M_{W\to jj}$ of the $m_{W\to jj}$ distribution derived from Monte Carlo simulations within the resolution $\sigma_{M_{W\to jj}}$. In the second term ΔM_t is the difference between the reconstructed mass of the semileptonically decaying top $m_{top\to b\ell\nu}$ and the mass of the hadronically decaying top quark $m_{top\to bjj}$. Since the two top quarks are identical particles, the mass difference of both reconstructed top quarks is assumed to be zero, within the uncertainty $\sigma_{\Delta M_t}$. P_{energy} is the fraction of the sum of transverse energies of the two top quarks and the total transverse energy of the event including missing transverse energy. The values for $M_{W\to jj}$, $\sigma_{M_{W\to jj}}$, $\sigma_{\Delta M_t}$, and α are obtained from MC studies.

Figure 2 provides the distributions for Ψ and its main ingredients χ^2 and $P_{\mathrm{b-light}}$ as measured in the data together with the the Monte Carlo expectation. Ψ is calculated for each hypothesis in the event and we then choose for each event the hypothesis with the smallest value of Ψ to get the reconstructed $cos\theta^*$ distribution (see figure 3).

6 Extraction of F_0 and F_+

For the extraction of the helicity fractions we perform a binned likelihood fit [7]. In two separate measurements we first measure F_0 and F_+ separately and therefore fix the respectively other fraction to its standard model value (F_0 is fixed to 0.7 for the measurement of F_+ and F_+ is fixed to 0.0 for the measurement of F_0). Thus only one free parameter is used in both fits. In a second measurement we fit both fractions simultaneously.

The likelihood function $L(a)$ (where "a" stands for the free parameter(s) - F_0, F_+, or both) is given by:

$$L(a,\beta) = e^{-\frac{(1-\beta)^2}{\sigma^2_\beta}} \cdot \prod_{k=1}^{Nbins} \frac{\mu_k^{\exp}(a,\beta)^{n_k} e^{-\mu_k^{\exp}(a,\beta)}}{n_k!} \tag{8}$$

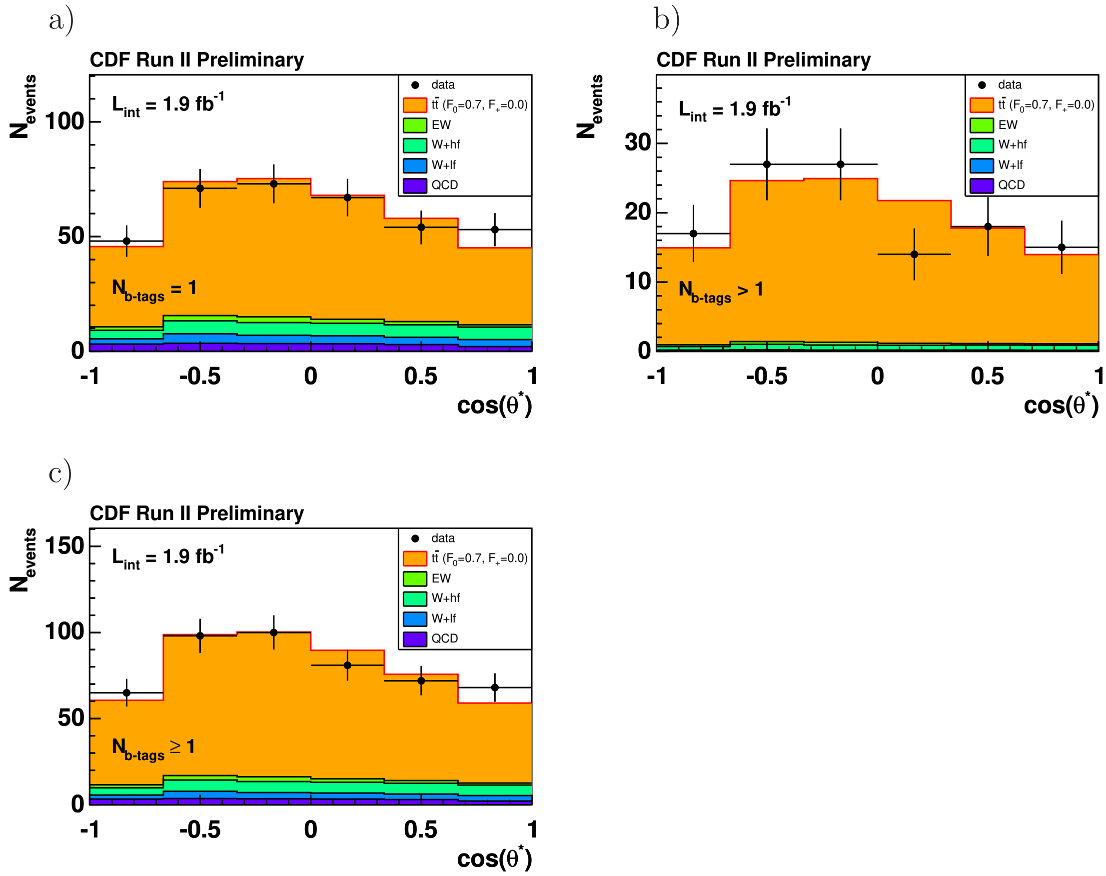

Figure 3: The reconstructed $\cos\theta^*$ distribution together with the SM expectation obtained from MC and the background model for the single-tag sample (a), the double-tag sample (b) and for the total data sample.

Here, μ_k^{exp} denotes the number of events expected to be observed in bin k of the reconstructed $\cos\theta^*_{\text{rec}}$ distribution and n_k the actually measured number of events in the same bin. The expected number of events μ_k^{exp} in bin k is the sum of the expected number of $t\bar{t}$ signal events $\mu_k^{\text{sig,exp}}$ and the expected number of background events $\mu_k^{\text{BG,exp}}$:

$$\mu_k^{\text{exp}}(a,\beta) = N_{sig} \cdot \hat{\mu}_k^{\text{sig,exp}}(a) + N_{BG} \cdot \hat{\mu}_k^{\text{BG,exp}}(a) \cdot \beta \tag{9}$$

The expected number of signal events in bin k is calculated via:

$$\hat{\mu}_k^{\text{sig,exp}} \propto \sum_i \mu_i^{sig}(F_0, F_+) \cdot \epsilon_i \cdot S(i,k) \tag{10}$$

considering acceptance and migration effects. The starting point is the theoretically predicted number of signal events in each bin $\mu_i^{sig}(F_0, F_+)$ which depends on F_0 and F_+ (the dependence on F_- is eliminated using the constraint $F_0 + F_+ + F_- = 1$). Since the event selection acceptance depends on $\cos\theta^*$ we apply for each bin a different event selection efficiency ϵ_i. The migration matrix S takes migration effects due to the finite resolu-

Source	1 parameter fit ΔF_0	1 parameter fit ΔF_+	2 parameter fit ΔF_0	2 parameter fit ΔF_+
MC Generator	0.012	0.005	0.015	0.002
Initial State Radiation	0.010	0.003	0.036	0.014
Final State Radiation	0.025	0.011	0.045	0.016
Jet Energy Scale	0.045	0.025	0.016	0.032
Background shape	0.032	0.019	0.028	0.032
Parton Distribution Function	0.005	0.002	0.014	0.006
Total	0.062	0.034	0.069	0.050

Table 1: Summary of systematic uncertainties, the total error is calculated by adding all single uncertainties in quadrature.

tion of detector and the reconstruction method into account. The matrix element $S(i,k)$ gives the probability for an event with true value of $\cos\theta^*$ in bin i to be reconstructed in bin k of the $\cos\theta^*$ distribution. $\hat{\mu}_k^{\mathrm{BG,exp}}$ is the normalized background estimation derived from the background template. $N_{BG}\cdot\beta$ is the total number of background events and is equal to the estimation in section 4 for $\beta = 1$. The term $e^{-\frac{(1-\beta)^2}{\sigma_\beta^2}}$ in the likelihood function is a Gaussian constraint on the mean number of background events. N_{sig} is the total number of expected signal events and is given by $N_{observed} - N_{BG}\cdot\beta$.

We calculate separate signal templates for events with exactly one b tag and events with more than one b tag. The background templates are also divided into two separate templates. Together with the background estimation and the event yield we calculate a likelihood function for the "1 tag events" and one for the "2 tag events". The combined likelihood function which is used to get the fit result is then given by the product of the two likelihood functions.

7 Systematic Uncertainties

The systematic uncertainties caused by the theoretical modelling and the experimental setup are studied performing 5000 pseudo experiments (PE). For most sources of systematic uncertainties the signal events are drawn from a MC signal sample which is effected by the systematic to be studied. The systematic uncertainty is then given by the difference between the mean fit result for the PE with the systematic-signal sample and the mean fit result for the PE with the default Pythia signal sample. The numbers are presented in table 1.

We estimate the possible bias from MC modelling of $t\bar{t}$ events by comparing HERWIG [8] and Pythia event generators. The influence of initial and final state radiation is estimated by comparing templates from Pythia MC simulations in which the parameters for gluon radiation are varied to produce either less or more initial or final-state radiation compared to the standard setup and compared to each other. The largest difference is than taken as the systematic uncertainty. The uncertainty due to the jet energy scale is quantified by varying that correction within one standard deviation in both the negative and positive direction. Since we have included a Gaussian constraint on the variation of the background rate in the likelihood fit, the uncertainty on the background estimation is already considered, we therefore only investigate the influence of the background shape. To estimate the contribution to the total systematic uncertainty that arises from the uncertainty on the PDF, we study the uncertainty from the variation of the 20 CTEQ6M eigenvectors. The uncertainty caused by the uncertainty on the top-quark mass is not stated separately, because the W boson helicity depends explicitly on the top quark mass. Instead, we present our measurement at a certain top mass, namely 175 GeV/c^2. In addition we checked the influence of differing values for the top quark masses. In the region of interest $\pm$ 5 GeV/c^2 around 175 GeV/c^2, our method reproduces well the predicted helicity fractions for these top masses. For the 1-parameter fit the total systematic uncertainty for the measurement of F_0 is 0.06, and 0.03 for the measurement of F_+. For the simultaneous fit the total uncertainty of F_0 is 0.07, and 0.05 for F_+.

8 Results

Performing the fit with fixed $F_+ = 0.0$ the fraction F_0 of longitudinally polarized W bosons is determined to be $F_0 = 0.66 \pm 0.10$ (stat) ± 0.06 (syst), which is within the uncertainty consistent with the standard model prediction of 0.7. Fixing F_0 to 0.7, we find $F_+ = 0.01 \pm 0.05$ (stat) ± 0.03 (syst), which is also consistent with the prediction of zero. The background parameter is $\beta = 1.02 \pm 0.20$ in both cases.

Since no evidence for a nonzero fraction of right handed W bosons is found, we calculate an upper limit $F_+^{\max}$ for F_+ at the 95% confidence level (C.L.). Therefore we convolute the likelihood function L(F_+) with a Gaussian with mean zero and width corresponding to the systematic uncertainty on F_+. Since a Bayesian approach is pursued, we then integrate only in the physical region $0 \leq F_+ \leq 0.3$ applying a prior distribution which is 1 in the interval [0,0.3] and zero elsewhere:

$$C.L.(F_+ \leq F_+^{max}) = \frac{\int_0^{F_+^{max}} L(F_+)dF_+}{\int_0^{0.3} L(F_+)dF_+} := 0.95 \tag{11}$$

We set an upper limit on the fraction of right-handed polarized W-bosons at the 95% confidence level of $F_+ < 0.12$, The probability density $P(F_+) = L(F_+)/\int_0^{0.3} L(F_+)dF_+$ is presented in figure 4c) and the region excluded at 95% confidence level is indicated in white.

In a second measurement we neither fix F_0 nor F_+ but fit both fractions simultaneously. For this measurement we find $F_0 = 0.38 \pm 0.21$ (stat) ± 0.07 (syst) and $F_+ = 0.15 \pm 0.10$ (stat) ± 0.05 (syst). The background parameter for this measurement is $\beta = 1.0 \pm 0.20$. The corresponding distribution of $-\Delta \ln L$ is shown in figure 5.

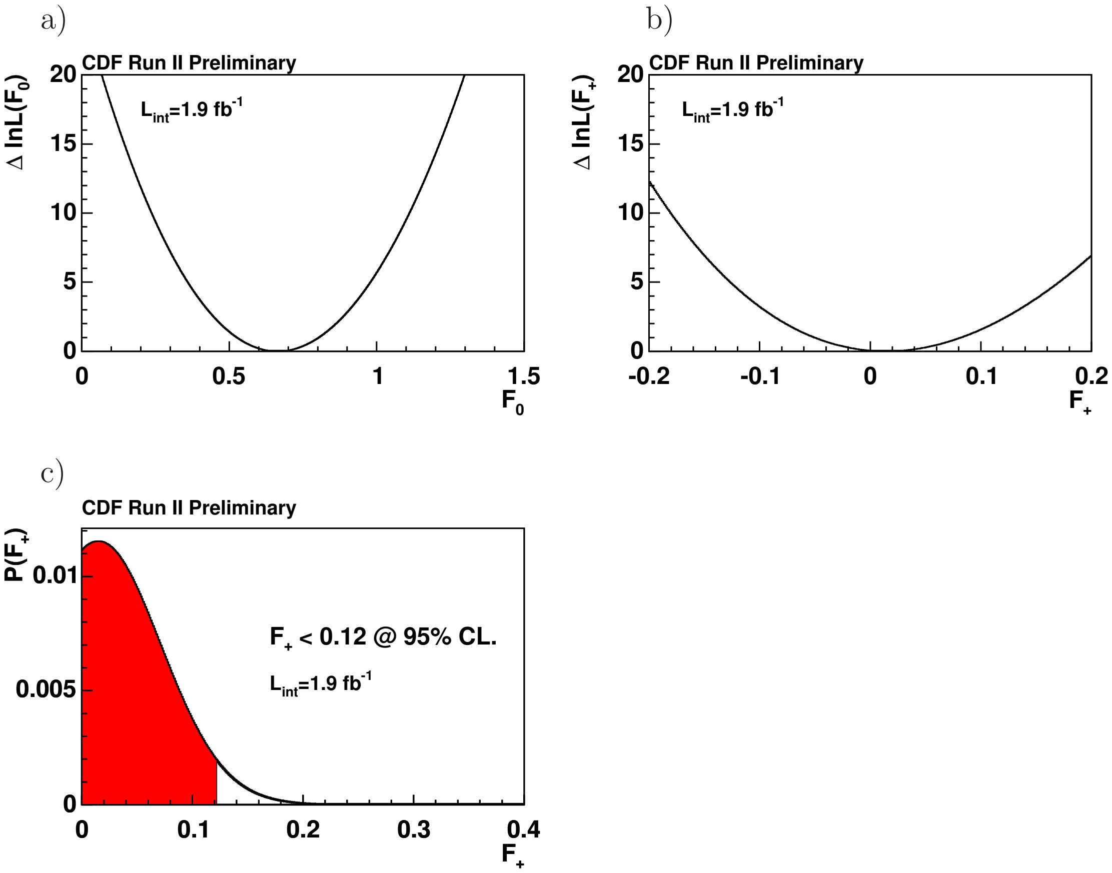

Figure 4: $\Delta \ln L$ as a function of a) F_0 and b) F_+.c) Posterior probability density as a function of F_+. The region excluded at the 95%C.L. is indicated in white.

Figure 6 shows the expected statistical uncertainty for the 1-parameter fit as well as for the 2-parameter fit obtained from pseudo experiments using MC generated events. Also the expected limit on F_+ is presented in this figure.

In order to allow a direct comparison of the $\cos\theta^*_{\rm rec}$ distribution obtained from the selected data sample with the calculated distributions for the different W boson helicity modes presented in figure 1, the background estimate is subtracted from the data. The shape of the $\cos\theta^*_{\rm rec}$ distribution is then corrected for acceptance effects as well as for resolution effects applying the transfer function $\tau(F_0, F_+)$.

Since the transfer function explicitly depends on F_0 and F_+ for the correction of the data distribution the specific transfer function for the F_0 value obtained by the likelihood fit has to be used, while the other parameter F_+ is set to its SM value, thus $\tau(F_0 = F_0^{\rm fit}, F_+ = 0)$. In a similar way the data can be corrected by using the result from the likelihood fit for F_+ and setting F_0 to its SM value, thus $\tau(F_0 = 0.7, F_+ = F_+^{\rm fit})$. It is also possible to use the results from the 2-parameter fit to calculate the transfer function.

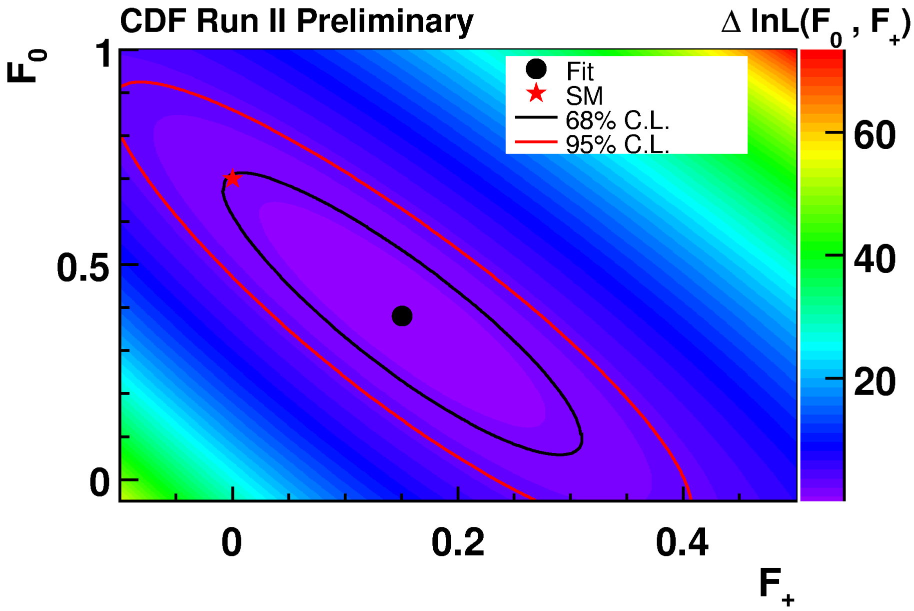

Figure 5: $\Delta \ln L$ for the 2-parameter fit. The SM prediction is indicated by the red star, the fitted result by the black point. The black line corresponds to the 68% CL. contour, the red line indicates the 95% CL. contour.

The value of the transfer function in the i^{th} bin of $\cos\theta^*$ is calculated from the normalized number of events $\hat{\mu}_i^{\text{sig}}$ before applying any selection cuts in the i^{ith} bin of $\cos\theta^*$ and from the normalized number of events $\hat{\mu}_k^{\text{sig,exp}}$ after applying the selection cuts and performing the reconstruction in the k^{th} bin of $\cos\theta^*_{\text{rec}}$:

$$\tau_i(F_0, F_+) = \frac{\hat{\mu}_i^{\text{sig}}(F_0, F_+)}{\hat{\mu}_{k=i}^{\text{sig,exp}}(F_0, F_+)} \quad . \tag{12}$$

Multiplying the background subtracted number of events in bin k ($k = i$) of $\cos\theta^*_{\text{rec}}$ with $\tau_i(F_0^{\text{fit}}, F_+ = 0)$, $\tau_i(F_0 = 0.7, F_+^{\text{fit}})$, or $\tau_i(F_0^{\text{fit}}, F_+^{\text{fit}})$ respectively and normalizing subsequently the corrected $\cos\theta^*$ data distribution to the theoretically calculated $t\bar{t}$ pair production cross section of $\sigma_{t\bar{t}} = 6.7 \pm 0.9$ pb [9, 10], leads to the desired distribution which is directly comparable with the theory distributions.

In figure 7 the corrected $\cos\theta^*$ distribution of the data normalized to the $t\bar{t}$ pair production cross section is presented. The uncertainty in the data is due to the uncertainty of the transfer function.

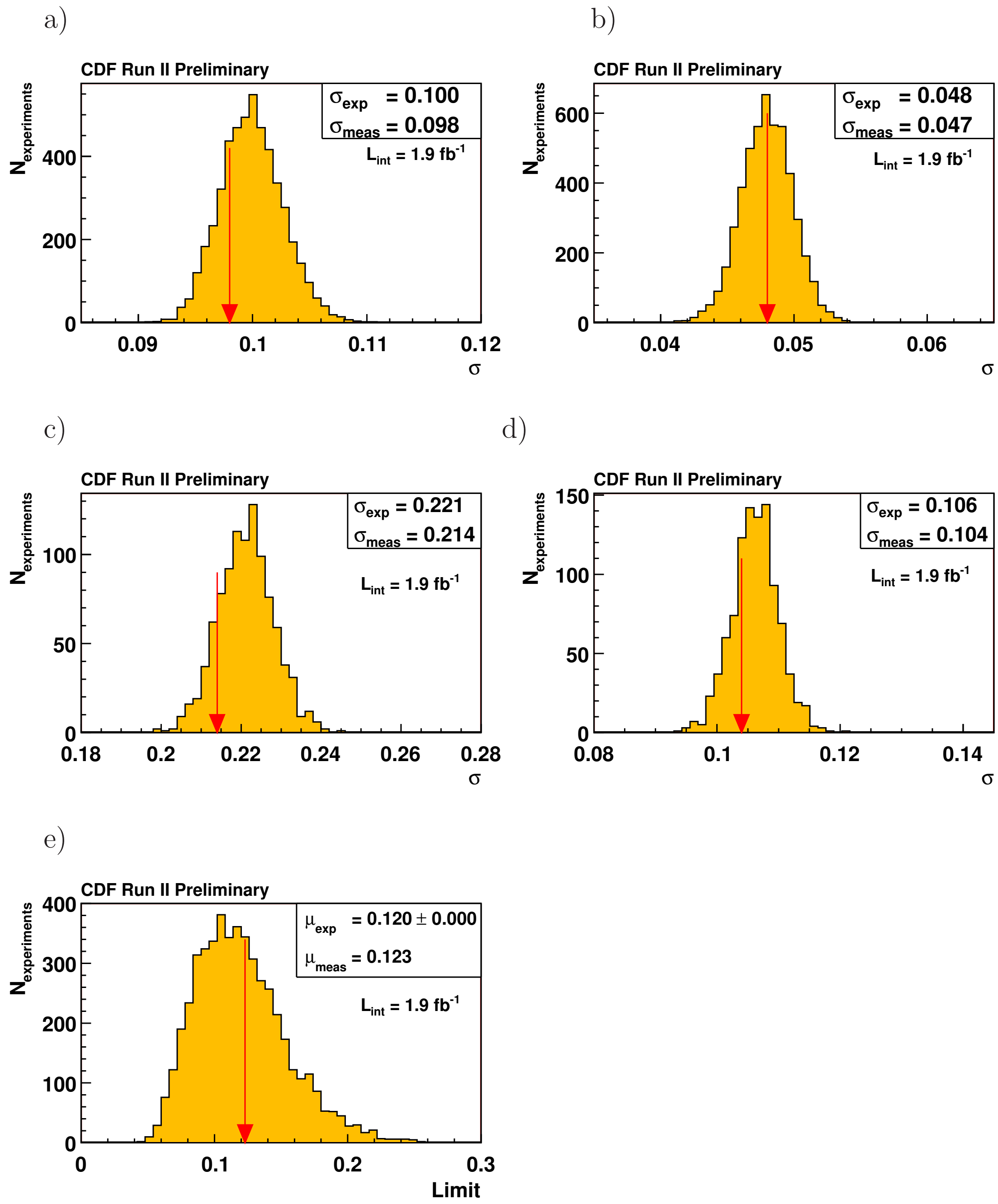

Figure 6: Expected statistical uncertainty together with the statistical uncertainty of the measurement (indicated by the red arrow) for the 1-parameter fit of F_0 (a) and of F_+ (b), and for the 2-parameter fit (c and d). e) Expected limit on F_+.

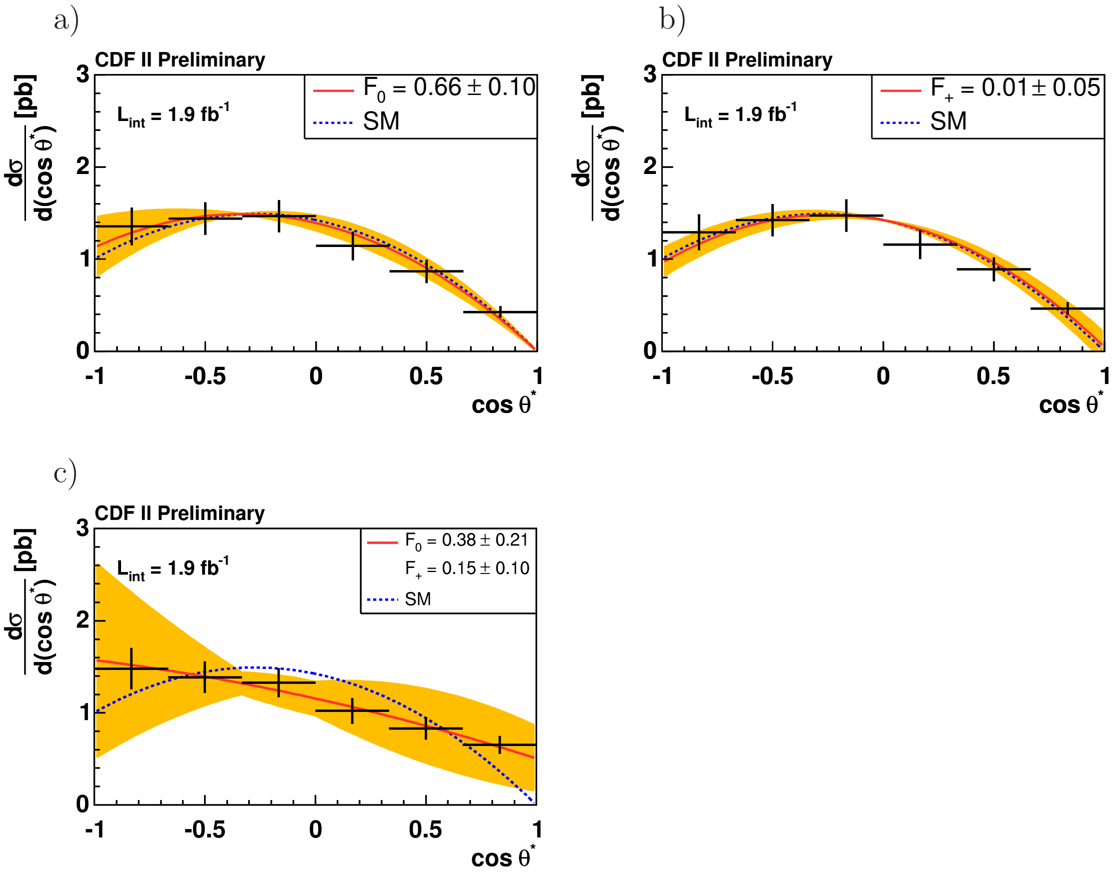

Figure 7: Unfolded $\cos\theta^*$ distribution in data normalized to the calculated $t\bar{t}$ cross section. a) shows the unfolded distribution derived by applying the transfer function obtained from the fitted value of $F_0 (F_+ = 0)$. In b) the fit result of F_+ ($F_0 = 0.7$) was used for the calculation of the transfer function. For c) the results from the 2-parameter fit were used. The red solid line represents the fit result, while the yellow band indicates the $\pm 1\sigma$ stat. uncertainty of the fit result. For comparison the blue dashed line shows the $\cos\theta^*$ distribution predicted by the standard model.

9 Summary

We presented a measurement of the fraction of longitudinally (F_0) and right-handed (F_+) polarized W bosons in top quark decays using an integrated luminosity of about 1.9 fb^{-1} collected at the CDF II detector. $t\bar{t}$ events have been selected, where one top quark decays semileptonically into a b quark, a charged lepton $\ell = e, \mu$ and a neutrino and where the other top quark decays hadronically (lepton + jets channel). Since a large discrimination between the three W helicities occurs in the cosine of the decay angle θ^* of the charged lepton in the W rest frame measured with respect to the W boson direction in the top rest frame, we use this quantity for the extraction of the W helicities. In order to determine the

$\cos\theta^*$ distribution in the data, the kinematics of the $t\bar{t}$ events is fully reconstructed and the best hypothesis is chosen. The helicity fraction F_0 is extracted under the assumption $F_+ = 0$ (Standard Model prediction) and the right-handed fraction is extracted under the assumption $F_0 = 70\%$ (SM prediction) using a binned maximum likelihood method and assuming a top quark mass of 175 GeV. We find

$$F_0 = 0.66 \ \pm 0.10 \text{ (stat)} \ \pm 0.06 \text{ (syst)} \quad (13)$$

$$F_+ = 0.01 \ \pm 0.05 \text{ (stat)} \ \pm 0.03 \text{ (syst)} \quad (14)$$

and set an upper limit on the fraction of right handed W bosons (for F_0 fixed to 0.7): $F_+ < 0.12\,@95\,\%\,CL$. Fitting both fractions simultaneously we find:

$$F_0 = 0.38 \ \pm 0.21 \text{ (stat)} \ \pm 0.07 \text{ (syst)} \quad (15)$$

$$F_+ = 0.15 \ \pm 0.10 \text{ (stat)} \ \pm 0.05 \text{ (syst)} \quad (16)$$

All results are within the uncertainties consistent with the standard model predictions.

10 Acknowledgments

We thank the Fermilab staff and the technical staffs of the participating institutions for their vital contributions. This work was supported by the U.S. Department of Energy and National Science Foundation; the Italian Istituto Nazionale di Fisica Nucleare; the Ministry of Education, Culture, Sports, Science and Technology of Japan; the Natural Sciences and Engineering Research Council of Canada; the National Science Council of the Republic of China; the Swiss National Science Foundation; the A.P. Sloan Foundation; the Bundesministerium für Bildung und Forschung, Germany; the Korean Science and Engineering Foundation and the Korean Research Foundation; the Particle Physics and Astronomy Research Council and the Royal Society, UK; the Russian Foundation for Basic Research; the Comisión Interministerial de Ciencia y Tecnología, Spain; in part by the European Community's Human Potential Programme under contract HPRN-CT-2002-00292; and the Academy of Finland.

References

[1] CDF Collaboration, F. Abe *et al.*, Phys. Rev. Lett. **74**, 2626 (1995);
DØ Collaboration, S. Abachi *et al.*, Phys. Rev. Lett. **74**, 2632 (1995).

[2] G. L. Kane, G. A. Ladinsky and C. P. Yuan, Phys. Rev. D **45** (1992) 124.

[3] D. Acosta *et al.*, Phys. Rev. D **71**(2005) 032001,

[4] T. Sjöstrand *et al.*, Comput. Phys. Commun. **135**, 238 (2001).

[5] A. Affolder *et al.* (CDF), Phys. Rev. D **71**(2001) 032002.

[6] S. Richter, "Search for electroweak single top-quark production with the CDF II experiment", FERMILAB-THESIS-2007-35 (2007)

[7] V. Blobel and E. Lohrmann, "Statistische und numerische Methoden der Datenanalyse", Teubner, Stuttgart/Leipzig (1998)

[8] HERWIG 6.5, G. Corcella, I.G. Knowles, G. Marchesini, S. Moretti, K. Odagiri, P. Richardson, M.H. Seymour and B.R. Webber, hep-ph/0011363, hep-ph/0210213.

[9] N. Kidonakis and R. Vogt, Phys. Rev. D **68**, 114014 (2003).

[10] M. Cacciari *et al.*, J. High Energy Phys. **0404**, 068 (2004).